Extremely vertical sidewall trench etching on silicon substrate and modelling etching using artificial neural network

To cite this article: Dongxun Yang *et al* 2019 *Mater. Res. Express* **6** 125902

Materials Research Express

PAPER

Extremely vertical sidewall trench etching on silicon substrate and modelling etching using artificial neural network

RECEIVED
29 August 2019

REVISED
24 October 2019

ACCEPTED FOR PUBLICATION
8 November 2019

PUBLISHED
20 November 2019

Dongxun Yang[1], **Jiashuai Wang**[1], **Rui Li**[1], **Yanqing Ma**[1,2,3] and **Lei Ma**[1,3]

[1] Tianjin International Center for Nanoparticles and Nanosystems, Tianjin University, Tianjin 300072, People's Republic of China
[2] State Laboratory of Precision Measuring Technology and Instruments, Tianjin University, Tianjin 300072, People's Republic of China
[3] Authors to whom any correspondence should be addressed.

E-mail: mayanqing@tju.edu.cn **and** lei.ma@tju.edu.cn

Keywords: ANN, vertical silicon trench, parameters control, CCP-RIE

Abstract

The control of etching parameters e.g. RF power, gas flow rate, chamber pressure and bias voltage is critical for the modern semiconductor fabrication industry. It is quite benefit to clarify the correlation between parameters and predict the etching results on both scientific research and industrial fabrication. In this paper, we performed a combination of experimental and machine learning analysis to understand the importance of each parameter and the correlation between them. SF_6 and O_2 was employed in order to investigate the optimal condition for Si trench etching with vertical sidewall based on capacitively coupled plasma reactive ion etching system (CCP-RIE). Scanning electron microscopy (SEM) and atom force microscope (AFM) were separately applied to characterize the etching profile and measure the etching depth. According to the experimental results, the optimal recipe of etching trench with vertical sidewall on silicon substrate is proposed to be a mixture of 30 sccm SF_6 flow rate and 20 sccm O_2 flow rate with 240 W RF power under the pressure of 5.6 Pa. Machine learning method of artificial neural network (ANN) was conducted to analyze the correlation between etching parameters. Levenberg-Marquart back propagation algorithm with sigmoid activation function is adopted to train the ANN model. Results show that the ANN model can predict the etching rate and etching profile accurately with 0.99154 R-Value. The relative importance of each parameter was also identified by using Random Forest algorithm. The gas flow rate of SF_6 is the most significant factor of etching rate, meanwhile the ratio of SF_6 to O_2 flow rate plays the most important role in etching profile control.

1. Introduction

Reactive ion etching (RIE) is widely applied in modern nano/micro-fabrication of semiconductor electronics [1], solar cell [2], micro-optical electro-mechanical systems (MOEMS) [3–5], micro-electronic mechanical systems (MEMS) [6–9], etc The mechanism of RIE is shown in figure 1. First, the glow discharge is generated from a radio frequency (RF) power and the gaseous precursors are dissociated into diverse species including active radicals, cations and electrons. Second, the radicals react with the substrate surfaces and the cations attack the surfaces under a bias voltage to form volatile production evacuated by pumping systems [10]. Capacitively coupled plasma etching system (CCP-RIE) and inductively coupled plasma etching system (ICP-RIE) are two main etching systems. Although ICP-RIE takes advantage of high etching rate and high etching directivity better than CCP-RIE, it is too expensive for common researchers to afford. Oppositely, the price of CCP-RIE is acceptable but the etching performance is unsatisfactory. Research confronts challenges in anisotropic etching profile control when using different RIE system. It would be quite useful to find the optimal recipe for CCP-RIE if relationships of etching parameters including the relative importance are summarized [11]. Due to the complex interaction and coupling effects among these etching parameters, it is still elusive to understand the relationships by using experimental method. Nevertheless, Artificial Neural Network (ANN) provides a great

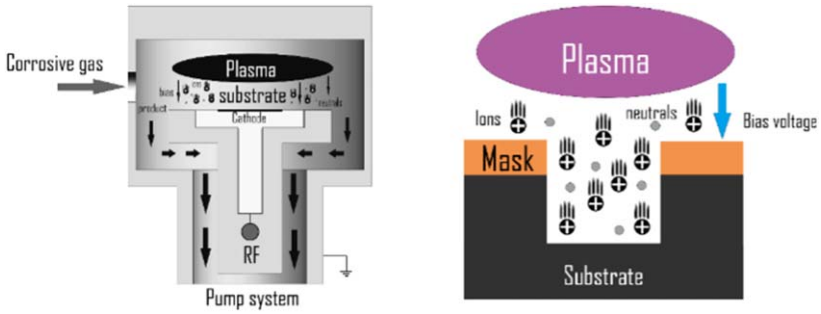

Figure 1. The illustration of reactive ion etcher.

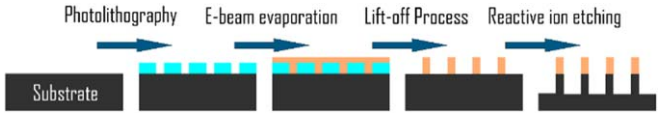

Figure 2. The illustration of sample preparation and fabrication.

promising method in solving multivariable problems and discovering the complex relationships without specific function mechanism [11, 12]. By learning from the experimental data, the ANN model can predict the etching rate and etching profile. In addition, the relative importance of parameters on etching rate and etching profile can also be clarified by using random forest algorithm [13].

In section 1, several experiments to study the influence of parameters such as RF power, gas flow rate, chamber pressure and gas ratios of SF_6 and O_2 flow rate on etching rate and etching profile of silicon (Si) are performed. The etching mechanism of each parameter during the etching process is discussed and the optimal recipe for etching trench with vertical sidewall is proposed based on the experimental results. In section 2, machine learning method to define the relationships of etching parameters is studied. A giant, predictable ANN model is generated based on Levenberg-Marquart algorithm learning from large experimental data. The relative importance of the parameters is calculated during the process by using random forest.

2. Experimental

Samples to be etched are fabricated in the same process, shown in figure 2. The metal masks are deposited by e-beam evaporation after patterned into stripes by photolithography. Ti/Ni (15 nm/25 nm) masks for silicon substrate are appropriate for the experiment. The etching process is carried out in reactive ion etching chamber (Tailong Electronics RIE-150) at a pressure below 4.92 Pa with SF_6 and O_2 supplied. Samples are characterized by scanning electron microscopy (Hitachi SU3500) to observe the etching profile, and by atomic force microscope (Parker NX10) to measure the etching depth in order to calculate the etching rate. All the bottom angle (theta) has been corrected by using Adobe Photoshop CC 2018.

3. Results and discussion

3.1. Parameters relationships in etching process on Si

High etching rate and anisotropic etching are two main advantages of reactive ion etching applied in micro-fabrication [14–16]. The combination of the chemical reaction and physical sputtering achieves anisotropic etching profile on many substrates including silicon [17, 18]. SF_6 and O_2 mixture gas has been widely used in etching silicon substrate for the advantage of high-speed etching rate and well directivity [19, 20]. During the etching process, RF power, total gas flow rate, ratios of SF_6 to O_2 gas flow rate and the chamber pressure are four main parameters in CCP-RIE system which take control of the density of etching radicals and bias voltage, furthermore, influencing the etching profile and etching rate [15]. Herein, the influence of these parameters on etching rate and especially the etching profile on silicon substrate is going to be discussed. With experimental results, an optimal recipe for etching extremely vertical trench on silicon is provided.

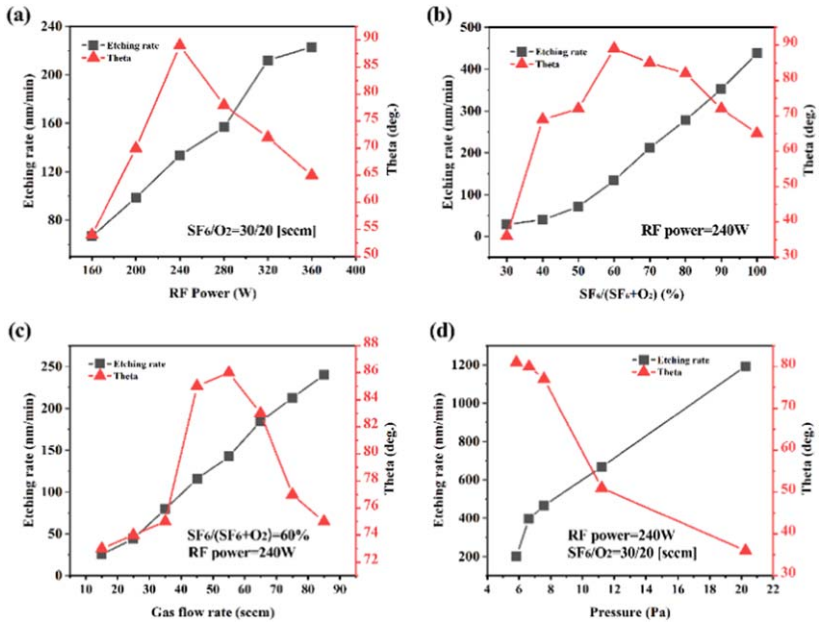

Figure 3. The variation of etching rate and etching profile with different etching parameters. (a) RF Power. (b) The ratio of SF_6/(SF_6 + O_2). (c) Total gas flow rate. (d) Pressure.

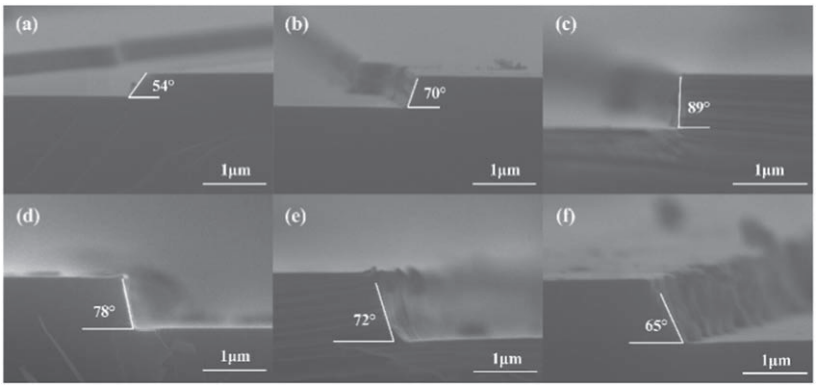

Figure 4. The SEM images of etching profile with different RF Power in condition of 30 sccm SF_6 with 20 sccm O_2. (a) 160 W, (b) 200 W, (c) 240 W, (d) 280 W, (e) 320 W, (f) 360 W. All scale bars are 1 μm.

In the CCP-RIE system, the RF power not only takes charge of the generation of plasma, but also provides the bias voltage, which means that the adjustment of the RF power can largely affect not only the chemical reactive between F radicals and Si substrate but also physical ion bombardment. Herein, the bottom angle of trenches (theta) is used to measure the perpendicularity of etching profile. The etching profile and etching rate of different RF power in the same condition are shown in figures 3(a) and 4. Results demonstrate the tendency of etching rate and etching profile with the variation of RF power. On the one hand, it is clearly indicated that etching rate is positively correlated with the RF power. It can be explained from the increasing of F radical density [19] and enhancement of ion bombardment. The effect of ion bombardment can be summarized into two parts. First, it provides defect sites for dissociative chemisorption and removes a monolayer of adsorbed gas on the surface that may prevent reaction. Second, the ion bombardment causes damage-enhanced diffusion and bond breaking generating unsaturated bonds. These unsaturated silicon bonds are easier to react with corrosive radicals such as fluorine to generate volatile product, leading the enhancement of etching rate [21]. On the other hand, the SEM images (figure 4) indicate the etching profile of trench under different RF power. It is seen that the sidewall of trench has been etched as bow-shaped above 240 W but as simply slope wall below 240 W. It implied the importance of RF power in adjusting the balance between chemical etching and physical ion bombardment in anisotropic etching process and the optimal RF power is 240 W. When RF power is below 240 W with constant gas flow rate of SF_6, a positive slope sidewall profile is observed in figures 4(a) and 5(b). It is presumably caused by sidewall passivation film forming and deposition during the etching process due to the weak ion

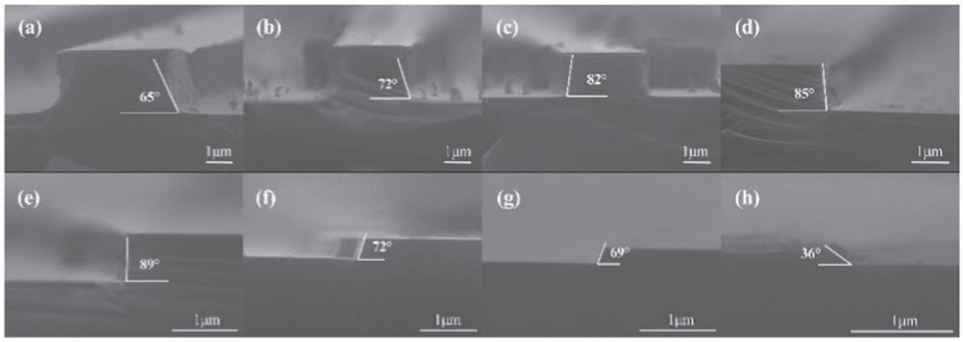

Figure 5. The SEM images of etching profile with different ratios of $SF_6/(SF_6 + O_2)$ in total gas flow rate of 50 sccm at 240 W. (a) 100%, (b) 90%, (c) 80, (d) 70%, (e) 60%, (f) 50%, (g) 40%, (h) 30%. All scale bars are 1 μm.

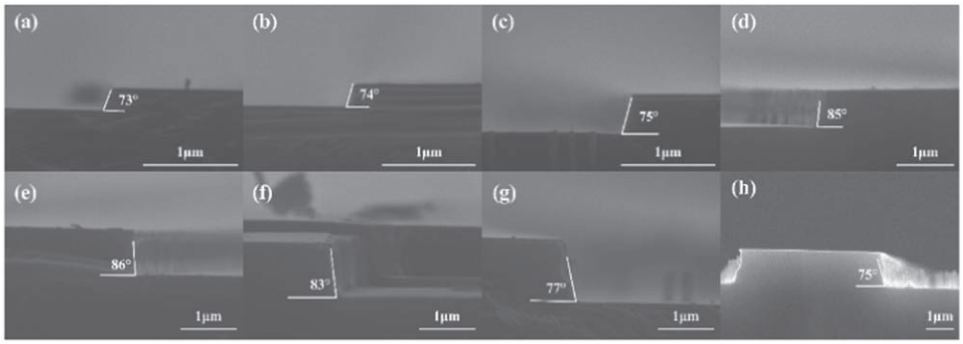

Figure 6. The SEM images of etching profile with different total gas flow rates in condition of 60% of $SF_6/(SF_6 + O_2)$ at 240 W. (a) 15 sccm, (b) 25 sccm, (c) 35 sccm, (d) 45 sccm, (e) 55 sccm, (f) 65 sccm, (g) 75 sccm, (h) 85 sccm.

bombardment [22]. However, when RF power is above 240 W with constant gas flow rate, the ion bombardment is getting much stronger so that the passivation of sidewall has been broken, leading a bow-shaped profile.

The ratio of SF_6 to O_2 is a key factor affecting both etching rate and etching profile. As shown in figure 3(b), the etching rate and bottom angle are varying with different percentage of SF_6. Obviously, the etching rate is mostly controlled by the percentage of SF_6 in the mixture gas for providing F radicals. When we improved the percentage of SF_6, the etching process is accelerated. Another interesting fact is that the ratio of SF_6 to O_2 flow rate dominated the perpendicularity of etching sidewall. It is indicated in figures 3(b) and 5 that the optimal ratio of $SF_6/(SF_6 + O_2)$ is 60% in order to obtain the most vertical sidewall profile. O_2 plays an important role during this selective etching process. There are two main roles of O_2 during the etching process. First, O_2 plays a role in adjusting the density of the chemical radicals in order to balance the chemical etching process and physical ion bombardment [15]. When the percentage of SF_6 is much larger than O_2, in the case of the strong chemical corrosion and declining of the bias voltage, the substrate beneath the mask is etched, resulting in an undercut profile. Second, O_2 helps passivate the sidewall from etching in generating passivation layer $Si_xO_yF_z$ so that the vertical sidewall can be obtained [15, 23, 24]. However, when the percentage of O_2 is much higher than SF_6, the etching rate slows down for both the passivation being occupied on the etching surface to prevent the target surface from chemical corrosion and dilution of F radicals [15]. Meanwhile, the profile of positive sloped sidewall is also formed at low $SF_6/(SF_6 + O_2)$ ratio, shown in figures 5(f)–(h). It is due to the strong passivation effect on sidewall with high percentage of O_2 [22].

In order to find out the influence of total gas flow rate on etching rate and etching profile in the optimal gas ratio of SF_6 to O_2, a series of gas flow rate have been used to etch Si in 240 W RF power. The experimental results are shown in figure 3(c) and SEM images are shown in figure 6. The etching rate linearly increases with the gas flow rate, as higher gas flow rate of SF_6 can provide more F radicals in chemical etching process [25]. According to the SEM images, all the bottom angles is greater than 73°, implying that the optimal ratio of SF_6 to O_2 certainly leads to the formation of relative vertical sidewall. It also shows a great anisotropic etching profile between 45 sccm to 55 sccm. Comparing with the experiment result in figure 3(c), the optimal gas flow rate should be 30 sccm SF_6 with 20 sccm O_2.

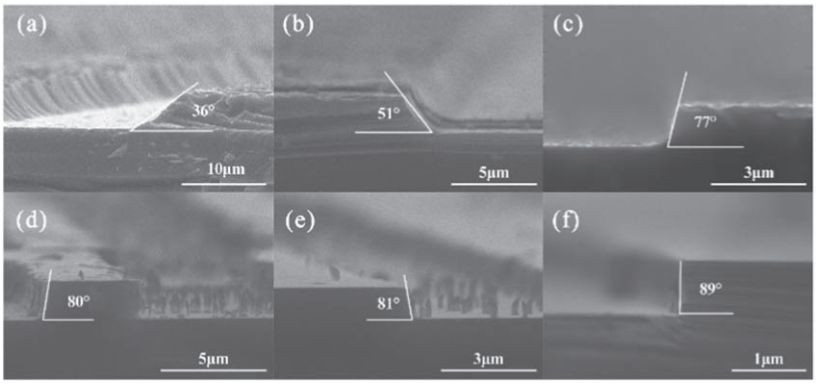

Figure 7. The SEM images of etching profiled with different pressure in condition of 30 sccm SF_6 with 20 sccm O_2 at 240 W. (a) 20.3 Pa, (b) 11.2 Pa, (c) 7.6 Pa, (d) 6.6 Pa, (e) 5.8 Pa, (f) 5.6 Pa.

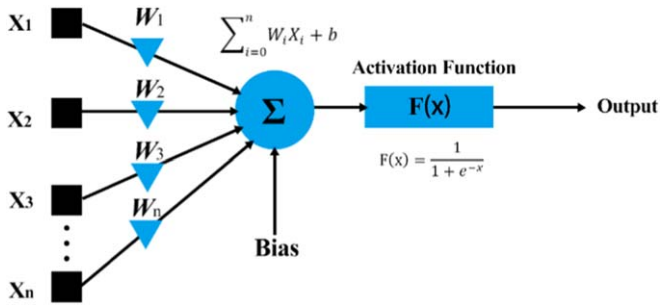

Figure 8. The mechanism of neutrons in ANN.

Table 1. The optimal recipe for etching vertical silicon sidewall.

SF_6	O_2	RF Power	Pressure	Etching rate	Theta
30 sccm	20 sccm	240 W	5.7 Pa	133 nm min^{-1}	89°

Besides the RF power, gas flow rate and gas ratio, the chamber pressure is another main factor taking control of the etching rate and etching profile [26]. However, limited by the structure of chamber, the adjustment of open value of high valve cannot give linear variety of chamber pressure. The pressure ranging is set from 5.8 Pa to 20.3 Pa to study the influence of chamber pressure. Results of etching rate and bottom angles are shown in figure 3(d) and SEM images are shown in figure 7. It is proved that an anisotropic etching profile is preferred in a lower chamber pressure and etching rate increases exponentially in high-pressure condition. For the purpose of achieving anisotropic etching, we prefer to keep the open value of high valve as a full open condition in order to obtain pressure as lowest as possible in Si etching process.

Finally, we analyze the influence of four main parameters on etching rate and etching profile. According to the experiment results, an optimal recipe for etching vertical sidewall on Si substrate has been summarized in table 1. However, experiments on these complicated multivariable problems are still very challenging. Based on the experimental result, machine learning provides a promising method to analyze the multivariable problems and show valuable reference on RIE practice.

3.2. ANN modelling and parameters relative importance analyzed by random forest

ANN is the most powerful machine learning method inspired by biological nervous system of humans [27]. Consisting of an input layer, hidden layers and an output layers, ANN exhibits significant performance in fast calculation and prediction application [12, 28, 29]. A system diagram for an artificial neural network is shown in figure 8. The operation mechanism is given by equation (1),

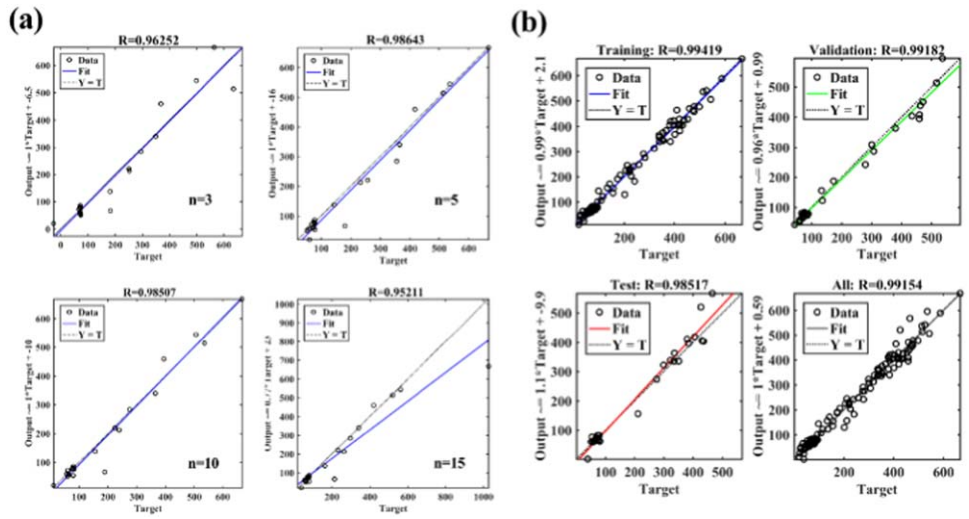

Figure 9. (a)The regression chart of test group with neutrons number of 3, 5, 10 and 15 in hidden layer. (b)The regression chart of ANN model with 10 neutrons in hidden layer.

$$y = \sum_{i=0}^{n} W_i X_i + b \tag{1}$$

where $X_i = (X_1, X_2, \ldots, X_n)$ represents the input applied to the neural and y is the output, $W_i = (W_1, W_2, \ldots, W_n)$ represents the weight for input and b represents the bias of the network [30]. Each neuron has an activation function as sigmoid nonlinear activation function (equation (2)), which determines the output data.

$$F(x) = \frac{1}{1 + e^{-x}} \tag{2}$$

This part is focus on the process of plasma etching on Si substrate and prediction of etching profile from the providing etching parameters. Based on Levenberg-Marquart back propagation algorithm with sigmoid nonlinear activation function, the structure of ANN is generated aiming at achieving great consistence with the experimental results and accuracy prediction. The seven input parameters are the gas flow rate of SF_6, the gas flow rate of O_2, total gas flow rate, the ratio of $SF_6/(SF_6 + O_2)$, pressure, RF power and V_{dc}. The output parameters are etching rate and bottom angle (theta). In order to avoid the problem of overfitting, the number of neutrons in hidden layers has to be bounded [31]. It is set the number of neutrons as 3, 5, 10 and 15. The R-Value of the test group is used to evaluate the fitting performance of ANN models. Regression R-Values measures the correlation between outputs and targets. An R-value of 1 represents a close relationship, 0 a random relationship. We list the regression chart of the test group in different neutron numbers of ANN models in figure 9(a). It is shown that the neutron numbers of 3, 5 and 10 have a great fitting performance but 15 is overfitting. Therefore, 10 neutrons in hidden layers is to generate our ANN model, the regression chart of 10 neutrons ANN model is shown in figure 9(b) and the R-Value of all data is 0.99154. The comparison between experiment and simulation of etching rate and bottom angle is shown in figures 10(a) and (b).

The method of Random Forests is a generalization of the decision tree method, in which multiple decision trees are built using random samples of observation for each tree and random samples of predictors [32]. Variable importance is assessed by randomly permuting the values of one predictor across all trees and estimating the loss in prediction accuracy of the forest. In other words, little loss implies low importance [33]. A special property of Random Forest is that the error rate will get smaller and smaller as more and more component predictors are added because the Random Forests method comes with a built-in protection against overfitting by using part of the data that each tree in the forest [32]. Thus, employing more component predictors will not lead to overfitting. Due to the great performance in calculating variable importance, Random Forests have been used in many field [34, 35]. One thing to be mention is that the variable importance can only be interpreted comparative to each other, rather than as absolute values [32]. Random Forest was used to analysis the relative importance of etching parameters on etching rate and anisotropic etching profile. Figures 10(c) and (d) demonstrate the relative importance of parameters on etching rate and etching profile, ranked in a descent order. According to the simulation results, the gas flow rate of SF_6 shows greatest important in etching rate and the ratio of SF_6 to O_2 are the most influencing parameter on etching profile. Tables 2 and 3 list the detailed proportion of these parameters on etching rate and etching profile relatively.

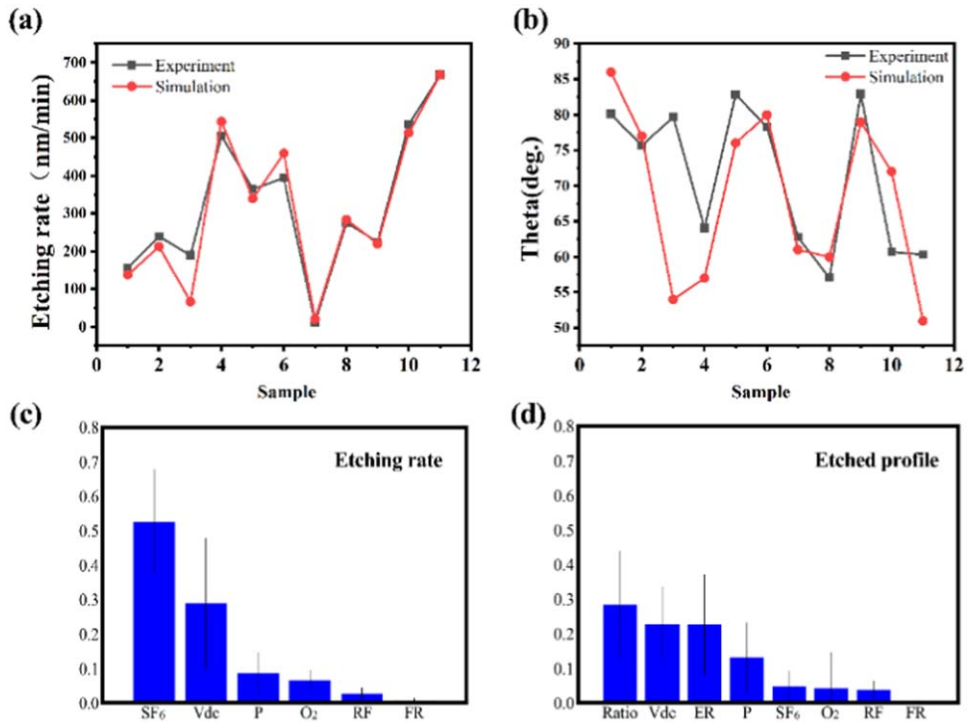

Figure 10. (a)The comparison of experiment results and simulation results in etching rate calculated by ANN model. (b) The comparison of experiment results and simulation results in etching profile calculated by ANN model. (c)The relative importance of parameters on etching rate calculated by Random Forest. (d)The relative importance of parameters on etching profile calculated by Random Forest. Abbreviations in the chart are explained in tables 2 and 3.

Table 2. The relative importance of etching parameters on etching rate.

P	SF_6	V_{dc}	P
RI	0.525881	0.288207	0.085855
P	O_2	RF	FR
RI	0.066023	0.027439	0.006595

P: Parameters; RI: Relative Importance; P: Pressure.
RF: RF Power; FR: Flow rate.

Table 3. The relative importance of etching parameters on etching profile.

P	Ratio	V_{dc}	ER	P
RI	0.283670	0.227271	0.226643	0.131072
P	SF_6	O_2	RF	FR
RI	0.047245	0.042466	0.038108	0.003525

P: Parameters; RI: Relative Importance; P: Pressure.
RF: RF Power; FR: Flow rate; ER: Etching rate.

4. Conclusion

In this paper, an optimal recipe using SF_6 and O_2 mixture gas on CCP-RIE for etching silicon trench with vertical sidewall has been summarized experimentally as 30 sccm SF_6 with 20 sccm O_2 in 240 W RF power at a full open high valve condition (5.6 Pa). By using the machine learning methods of ANN and Random Forest, the relationships of etching parameters including RF power, the chamber pressure, the gas ratio of SF_6 to O_2 and the

total gas flow rate have been studied. A predictable ANN model is generated by using MATLAB neural network fitting toolbox based on Levenberg-Marquardt with sigmoid nonlinear activation function.10 neutrons has been set in hidden layers in order to achieve the best performance and to avoid overfitting. Besides that, the relative importance of each parameter on etching rate and etching profile has been calculated by using Random Forest algorithm. Results show the gas flow rate of SF_6 is the most significant factor on etching rate. The ratio of SF_6 to O_2 is the greatest influencing parameter on etching profile.

Acknowledgments

Funding: This study was funded by the National Natural Science Foundation of China (No. 11774255) and the Key Project of Natural Science Foundation of Tianjin City (No. 17JCZDJC30100).

Conflict of interest

The authors are all in Tianjin International Center for Nanoparticles and Nanosystems. And declare that they have no conflict of interest.

ORCID iDs

Yanqing Ma https://orcid.org/0000-0002-3317-8273

References

[1] Pu T, Wang X, Huang Q, Zhang T, Li X, Li L and Ao J-P 2019 *IEEE Electron Device Lett.* **40** 185
[2] Ahn S *et al* 2019 *J. Phys. D: Appl. Phys.* **52** 035502
[3] Teo A J T, Li H K-H, Tan S H and Yoon Y-J 2018 *Microsyst. Technol.* **24** 465
[4] Teo A J T, Li H, Tan S H and Yoon Y-J 2017 *J. Micromech. Microeng.* **27** 067001
[5] Fan J, Zhang W T, Liu J Q, Wu W J, Zhu T and Tu L C 2015 *J. Micro/Nanolithogr. MEMS MOEMS* **14** 024502
[6] Cao H *et al* 2019 *Micromachines (Basel)* **10** 186
[7] Mansoor M, Haneef I, De Luca A, Coull J and Udrea F 2018 *J. Micromech. Microeng.* **28** 085013
[8] Zhang X, Yu X, Li T and Wang Y 2018 *Microsyst. Technol.* **24** 2913
[9] Kim J W, Kim K B, Kim J H and Min N K 2018 *J. Micromech. Microeng.* **28** 125004
[10] Coburn J W and Winters H F 1979 *J. Vac. Sci. Technol.* **16** 391
[11] Pankajakshan P, Sanyal S, de Noord O E, Bhattacharya I, Bhattacharyya A and Waghmare U 2017 *Chem. Mater.* **29** 4190
[12] Witek-Krowiak A, Chojnacka K, Podstawczyk D, Dawiec A and Pokomeda K 2014 *Bioresour. Technol.* **160** 150
[13] Svetnik V, Liaw A, Tong C, Culberson J C, Sheridan R P and Feuston B P 2003 *J. Chem. Inf. Comput. Sci.* **43** 1947
[14] Nojiri K 1996 *J. Vac. Sci. Technol., B* **14** 1791
[15] Jansen H, Gardeniers H, Boer Md, Elwenspoek M and Fluitman J 1996 *J. Micromech. Microeng.* **6** 14
[16] Pandhumsoporn T, Wang L, Feldbaum M, Gadgil P, Puech M and Maquin P 1998 *Smart Structures and Materials 1998: Smart Electronics and MEMS* **3328** 93
[17] Mansano R D, Verdonck P, Maciel H S and Massia M 1999 *Thin Solid Films* **343–344** 378
[18] Yunkin V A, Fischer D and Voges E 1994 *Microelectron. Eng.* **23** 373
[19] Alshaltami K A and Daniels S 2019 *AIP Adv.* **9** 035047
[20] d'Agostino R and Flamm D L 1981 *J. Appl. Phys.* **52** 162
[21] Coburn J W and Winters H F 1979 *J. Appl. Phys.* **50** 3189
[22] Donnelly V M and Kornblit A 2013 *Journal of Vacuum Science & Technology A: Vacuum, Surfaces, and Films* **31** 050825
[23] Mellhaoui X, Dussart R, Tillocher T, Lefaucheux P, Ranson P, Boufnichel M and Overzet L J 2005 *J. Appl. Phys.* **98** 104901
[24] Atteia F, Rouzo J and Berginc G 2019 *Physics, Simulation, and Photonic Engineering of Photovoltaic Devices VIII, Proc. SPIE* **10913** 109130U-1
[25] Gray D C, Tepermeister I and Sawin H H 1993 *J. Vac. Sci. Technol., B* **11** 1243
[26] Kim B and Lee B-T 2013 *Surf. Eng.* **20** 391
[27] Saad Saoud L and Khellaf A 2010 *Neural Computing and Applications* **20** 329
[28] Mohanraj M, Jayaraj S and Muraleedharan C 2015 *Int. J. Therm. Sci.* **90** 150
[29] Dongale T D, Jadhav P R, Navathe G J, Kim J H, Karanjkar M M and Patil P S 2015 *Mater. Sci. Semicond. Process.* **36** 43
[30] Hameed A A, Karlik B and Salman M S 2016 *Knowl.-Based Syst.* **114** 79
[31] Jin L, Kuang X, Huang H, Qin Z and Wang Y 2005 *Acta Meteorol. Sin.* **19** 216
[32] Matsuki K, Kuperman V and Van Dyke J A 2016 *Scientific Studies of Reading* **20** 20
[33] Oh J, Laubach M and Luczak A 2003 Estimating neuronal variable importance with random forest *IEEE Bioengineering Conf.*. 33–34
[34] Hallett M J, Fan J J, Su X G, Levine R A and Nunn M E 2014 *Statistical Modelling* **14** 523
[35] Gazzola G, Choi J, Kwak D-S, Kim B, Kim D M, Tong S H and Jeong M-K 2018 *IEEE Trans. Semicond. Manuf.* **31** 343